ACS OMEGA

http://pubs.acs.org/journal/acsodf

Article

C-4-Modified Isotetrones Prevent Biofilm Growth and Persister Cell Resuscitation in *Mycobacterium smegmatis*

Kingshuk Bag, Aditya Kumar Pal, Subhadip Basu, Mamta Singla, Biplab Sarkar, Dipankar Chatterji, Prabal Kumar Maiti,* Anirban Ghosh,* and Narayanaswamy Jayaraman*

Cite This: *ACS Omega* 2023, 8, 20513−20523

Read Online

ACCESS | Metrics & More | Article Recommendations | Supporting Information

ABSTRACT: Hyperphosphorylated nucleotide (p)ppGpp, synthesized by Rel protein, regulates the stringent response pathway responsible for biofilm and persister cell growth in mycobacteria. The discovery of vitamin C as an inhibitor of Rel protein activities raises the prospect of tetrone lactones to prevent such pathways. The closely related isotetrone lactone derivatives are identified herein as inhibitors of the above processes in a mycobacterium. Synthesis and biochemical evaluations show that an isotetrone possessing phenyl substituent at *C*-4 inhibit the biofilm formation at 400 μg mL^{-1}, 84 h post-exposure, followed by moderate inhibition by the isotetrone possessing the *p*-hydroxyphenyl substituent. The latter isotetrone inhibits the growth of persister cells at 400 μg mL^{-1} f.c. when monitored for 2 weeks, under PBS starvation. Isotetrones also potentiate the inhibition of antibiotic-tolerant regrowth of cells by ciprofloxacin (0.75 μg mL^{-1}) and thus act as bioenhancers. Molecular dynamics studies show that isotetrone derivatives bind to the Rel$_{Msm}$ protein more efficiently than vitamin C at a binding site possessing serine, threonine, lysine, and arginine.

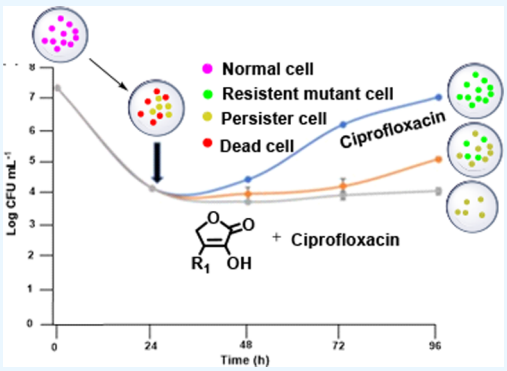

INTRODUCTION

Persister cells form a group of an antibiotic-tolerant bacterial cell population responsible for the resurgence of pathogenic infections upon withdrawal of antibiotics on infected host cells.[1] Among other factors, the stringent response pathway regulates the persister cell emergence and the pathway is regulated heavily by hyperphosphorylated guanosine nucleotides, namely, (p)ppGpp.[2−7] Sustained investigations show the intense inter-relationship of mycobacterial stringent response pathway, persister cell formation, and infection to the host cells by overcoming antibiotic treatments.[8−12] The emergence of persister cells is often correlated to the synthesis of (p)ppGpp by Rel, which is a predominant bacterial enzyme. Under stress, such as, in starvation conditions, the Rel enzyme activates the (p)ppGpp synthesis, which, in turn, leads to persister cell growth, possessing altered metabolic processes. Targeting the stringent response pathway, and thus the (p)ppGpp synthesis, appears to be a promising approach to overcome persister cell-mediated infections to host cells.

Relacin and derivatives thereof have been developed as potent Rel inhibitors, although their in vivo inhibition activities occur in millimolar ranges.[13−15] Among other potent inhibitors studied so far, vitamin C shows promising inhibitory activities by inhibition of the ppGpp synthesis.[11] Vitamin C binds directly to the Rel enzyme and inhibits (p)ppGpp biosynthesis, thereby establishing the importance of vitamin C to prevent mycobacterial persister cell emergence. The inhibition of (p)ppGpp biosynthesis occurs at millimolar concentrations of vitamin C, although such high concentrations of vitamin C would not be an impediment to a normal course of administration to antibiotic-tolerant infected cells populated with persisters. Vitamin C has also been discovered recently as a potent inhibitor of persister cell growth in *M. smegmatis* and *M. tuberculosis* bacterial species.[16−21] These discoveries prompt studies of newer chemical entities possessing the tetrone lactone scaffold. Vitamin C is a tetrone lactone[22] and thus scaffold search of potential inhibitors with a varied substituent on the tetrone lactone is a viable approach. The present report demonstrates the potencies of newly formed *C*-4 modified isotetronic acids as inhibitors of *M. smegmatis* persister cell growth through a series of biochemical evaluations.

RESULTS AND DISCUSSION

Chemical Synthesis of *C*-4-Modified Isotetronic Acids. α-hydroxy-γ-butyrolactones, namely, isotetrone lactones form as a scaffold for many important natural products of therapeutic importance.[23−27] Many natural products possess

Received: February 8, 2023
Accepted: April 28, 2023
Published: May 31, 2023

the α-hydroxy-γ-butyrolactone scaffold.[28−34] Early biosynthesis studies by Yamamoto and co-workers demonstrated that α-amino acids form the substrate for the formation of α-hydroxy-γ-butyrolactone metabolites, produced during the culture growth of fungus *Aspergillus terreus* IFO 8835 strain.[35] The deamination of α-amino acids was presumed to form the first of several steps, leading to isotetrone formation. The deamination process led to the transformation of the α-amino acid to α-keto acid, namely, pyruvic acid. Pyruvic acid acts as an excellent nucleophile to aldol reactions with carbonyl electrophiles and in biosynthesis, and the reaction is mediated by a type II aldolase enzyme.[36,37] Subsequent lactonization leads the resulting cross-aldol product to the isotetrone. Pyruvic acid as an important synthon is well-exploited in the chemical synthesis of many derivatives of isotetrone, with substitutions at *C*-3 to *C*-5 carbons.[38−40] Enantioselective synthesis led to a paradigm shift and syntheses of stereochemically pure butyrolactones are also achieved.[41−49] Recognizing the importance of deamination of amino acids to the corresponding substituted pyruvic acids, we undertook to synthesize isotetrones that possess variations of the substituent at *C*-4 carbon of the furanone scaffold.

A facile approach to deamination of L-amino acid is considered as an important strategy, in order to enable the incorporation of substituents at the *C*-4 position of isotetrone.[50] The reaction of L-amino acids **1**−**3**, leucine, phenylalanine, and tyrosine, respectively, with trifluoroacetic anhydride, at optimal conditions of 85 °C and 1.5 h duration, afforded oxazolones **4**−**6** (Scheme 1), in good to moderate

Scheme 1. Synthesis of Isotetrones 10−12, from a-Amino Acids 1−3, through Oxazolones 4−6 and *C*-3 Substituted Pyruvic Acid 7−9 Intermediates

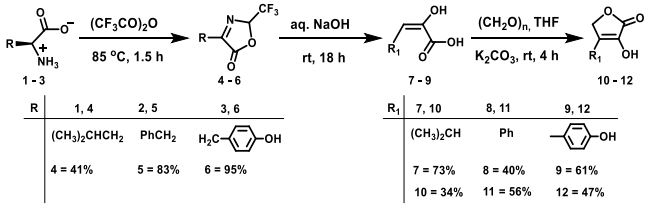

yields, in addition to the formation of trifluoroacetyl amino acids.[51,52] Oxazolones **4**−**6** were subjected to aq. alkaline hydrolysis at room temperature for 18 h and the corresponding pyruvic acids **7**−**9** formed, possessing either keto- or the enol ether functionality.[53,54] Enolization was observed higher in products **8** and **9**.

The reaction of pyruvic acids **7**−**9** with formalin for 4 h, in the presence of K_2CO_3, in THF, initiated the aldolization and subsequent lactonization of the cross-aldol intermediate during acidic work-up that led to the formation of isotetrones **10**−**12**. When the reaction was left for a longer duration, a double aldolization product was also noticed in the crude reaction mixture, particularly, with pyruvic acid intermediate derived from isoleucine **1**, whereas unreacted starting materials **4**−**6** remained when aldolization reactions were conducted for a shorter duration. The identities and structural homogeneities of intermediates **4**−**9** and final products **10**−**12** were ascertained by nuclear magnetic resonance (NMR) spectroscopies and mass spectrometry.

A similar reaction sequence was extended to valine, isoleucine, and tryptophan amino acids. Oxozolone formation, hydrolysis to the corresponding pyruvic acid derivatives,[55−57] aldolization with formalin, in the presence of K_2CO_3 and subsequent lactonization led to the formation of isotetrones **13**−**15** (Figure 1). In the case of valine, intermediate α-keto-γ-

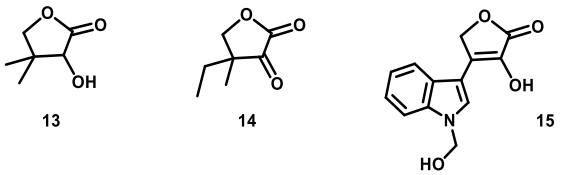

Figure 1. γ-Butyrolactones **13** and **14**, and isotetronic acid **15** synthesized from valine, isoleucine, and tryptophan, respectively.

butyrolactone was observed to undergo a further reduction in the presence of formalin so as to afford α-hydroxy-γ-butyrolactone **13**, which is a pantolactone. Such a transformation was not observed with butyrolactone **14**, derived from isoleucine. Additional hydroxymethylation also occurred at the indole−nitrogen of tryptophan-derived butyrolactone **15**. Characterizations of products **13**−**15** were established by NMR spectroscopies and mass spectrometry.

Each one of the isotetrones differ at the substituent nature at the *C*-4 carbon of the scaffold. Aromatic substituents possess variations, namely, phenolic, indole, and phenyl moieties as the substituent in one series. Aliphatic series possesses methyl, ethyl, and isopropyl substituents in a quaternary carbon. Isotetrone further was presented either in a keto or enol or a hydroxy functionality at the *C*-3 carbon. These functionalities represent the variations at each series of the scaffold.

Specific Isotetrones Interfere with Planktonic Growth of *M. smegmatis*. The studies were undertaken with fast-growing *M. smegmatis* acid-fast bacterium. Of the six *C*-4 modified isotetrones **10**−**15**, preliminary screening of the effects on planktonic growth of the bacterium showed isotetrones **11** and **12** showed inhibitory properties and these derivatives were shortlisted for further studies. Isotetrone **11** showed significant growth inhibition at the early exponential and late exponential phases compared to the untreated controls (Figure 2a).

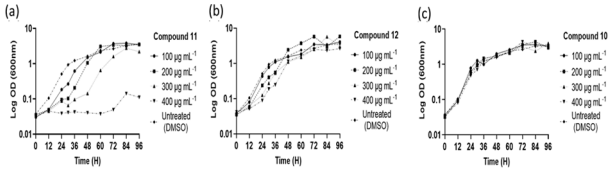

Figure 2. *M. smegmatis* growth curves in the presence of varying concentrations of (a) **11**; (b) **12**; and (c) **10**.

Further analysis showed that derivative **11** inhibited the bacterial planktonic growth in a dose-dependent manner, and at 400 μg mL^{-1}, complete growth inhibition occurred up to 72 h. After this duration, regrowth of cells was observed. A moderate growth inhibition was observed for isotetrone **12** during the exponential growth phase of *M. smegmatis* cells in a concentration-dependent manner (Figure 2b). In this instance too, cells tended to recover from the early inhibition in the exponential phase and growth similar to untreated control was observed by 60−72 h, indicating a transient inhibitory effect of these isotetrones. Isotetrone **10** did not intervene in the growth profile of *M. smegmatis* cells across all concentrations

https://doi.org/10.1021/acsomega.3c00822
ACS Omega 2023, 8, 20513−20523

when compared to the untreated control (Figure 2c). These differences in the growth profiles indicate that both the isotetrones **11** and **12** possessing an aromatic moiety at *C*-4 carbon act as transient bacterial growth inhibitors. Furthermore, the minimum inhibitory concentration (MIC) was checked for compound 11 and compound 12, and it was found to be 400 μg mL^{-1}.

Isotetrones Showed a Differential Killing Pattern in *M. smegmatis*. The transient growth inhibition prompted us to verify the effects of isotetrones in combination with a known antimicrobial drug.[58,59] A clinically relevant fluoroquinolone series drug, namely, ciprofloxacin (Cip), having a low MIC value against *M. smegmatis*, was chosen for this purpose. The initial determination of the MIC of Cip, in the presence of derivatives **10**−**12** (200 μg mL^{-1}), showed the following trend: Cip: 0.25 μg mL^{-1}; Cip + **10**: 0.25 μg mL^{-1}; Cip + **11**: 0.125 2 μg mL^{-1}; and Cip + **12**: 0.5 μg mL^{-1}.

In order to assess the efficacies of isotetrones to kill *M. smegmatis* WT cells, in MB7H9 media, a kill kinetics assay was conducted, either alone or in combination with ciprofloxacin. Isotetrone derivatives alone did not result in any drop in CFU mL^{-1}, implying that the derivatives lacked activity to kill the cells (Figure S13). An alternating killing pattern emerged when the cells were treated with a combination of ciprofloxacin (2.5 μg mL^{-1}) and different isotetrones (400 μg mL^{-1}). The drug in combination with **10** did not lead to any appreciable change in the killing, whereas ciprofloxacin (2.5 μg mL^{-1}) and isotetrone **11** and **12** combinations led to an antagonistic response, where the combinations led to a reduced killing at each plating time point (Figure 3). We presume the intrinsic growth inhibitory properties of **11** and **12** interfered with ciprofloxacin activity, leading to the differential killing of the replicating cells.

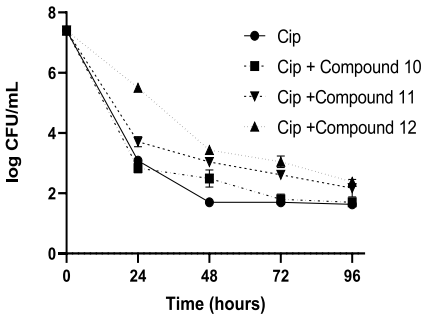

Figure 3. Kill kinetics of *M. smegmatis* with ciprofloxacin (Cip) (2.5 μg mL^{-1}) and Cip in the presence of derivatives **10**−**12** (400 μg mL^{-1}).

Selective Isotetrones Affect the Biofilm Formation of *M. smegmatis*. Vitamin C is the first tetronic acid derivative demonstrated to exhibit inhibitory activity against biofilm-grown mycobacterium, occurring at a concentration of ∼10 mM.[22] It was also assessed to interfere with the ppGpp biosynthesis in *M. smegmatis* and the biofilm growth.[18,60−62] Isotetrones synthesized in the present work were assessed for the inhibition of biofilm formation at the maturation stage of *M. smegmatis*. The biofilm morphologies were monitored for 84 h post-exposure to **10**−**12**. Among the derivatives, **11** showed the largest effect in a concentration-dependent manner (Figure 4). Derivative **12** showed moderate inhibition of the biofilm and derivative **10** did not show inhibition of biofilm, as

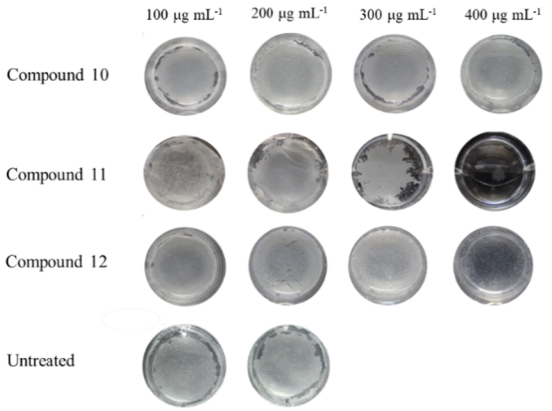

Figure 4. Images of *M. smegmatis* biofilms after 84 h, in the presence of varying concentrations of compounds **10**−**12** with untreated control.

that of the dense mature biofilm formed with untreated control (Figure 4).

Isotetronic Acids 11 and 12 Intercepts with Persister Population Regrowth and Resistant Mutant Enrichment at Low Ciprofloxacin Concentration. Earlier studies show that vitamin C targets the (p)ppGpp biosynthesis. The (p)ppGpp alarmone promotes the persister cell formation and plays a role in the antibiotic tolerance of the growing bacterium.[64,65] Given this, further experiments were performed to identify whether selected isotetrones would intercept the persister population dynamics and resistant mutant enrichment at low ciprofloxacin concentration. In laboratory and clinical settings, antibiotic treatment often leads to a biphasic response, with a rapid killing phase followed by a plateau, which is represented by a 0.01−0.001% nongrowing persister population. These antibiotic-tolerant persister cells lead to a major threat to effective antibiotic therapy, due to a resuscitation of the persisters into normal growing cells at a point soon after the antibiotic treatment is terminated, which results in recurrent infection. It is thus of interest to identify the effect of the isotetronic acids, specifically that 11 and 12, if these derivatives would possess a restrictive effect on the regrowth of the persister-dominated antibiotic-survived population, in the presence of a lower concentration of ciprofloxacin (0.75 μg mL^{-1}, which is 3 times higher than MIC). The lower concentration of the drug was chosen as our data indicated that the regrowth phenotype of drug-tolerant cells was very prominent at this concentration (Figure S14a) as well as genetic mutant enrichment (Figure S14b). Furthermore, the lower antibiotic concentration is very much relevant from a clinical perspective when optimum concentration could not be maintained. Next, the persister regrowth in the presence of isotetrones **11** and **12** was checked. In this assay, cells were treated first with the drug (0.75 μg mL^{-1}) for 24 h, thereby achieving ∼99.99% killing of the cells, leaving a residual ∼0.01% persister population retained in the culture. We measured the ciprofloxacin activity after 24 h of killing by a growth bioassay where it is shown that the culture filtrate retains the same active ciprofloxacin concentration for up to 96 h (Figure S16). In order to make sure the residual 0.01% after 24 h of ciprofloxacin treatment are bonafide persisters and not resistant mutants, the plating was done in MB + Cipro plates and hardly any resistant mutants were detected. By patching individual colonies of ciprofloxacin survived population in a 5X

https://doi.org/10.1021/acsomega.3c00822
ACS Omega 2023, 8, 20513−20523

ciprofloxacin plate, we confirmed ∼90% of the cells were persisters and ∼10% of the cells were resistant mutants (Figure S17). At this point, the culture was divided into three portions, added with either derivative **11** or **12** (400 μg mL^{-1}) and an equal volume of sterile milli-Q water. The growth kinetics was subsequently monitored, a brief nongrowing phase of approximately 24−36 h was observed first, and then, antibiotic-survived cells started to grow, as evident by the increase in CFU mL^{-1} at later time points. The data suggested significant prevention of the regrowth phase and a general delayed resuscitation of tolerant cells, in the presence of isotetrones **11** and **12** (400 μg mL^{-1}). As shown in the resuscitation growth curve (Figure 5a) between 48 and 72 h,

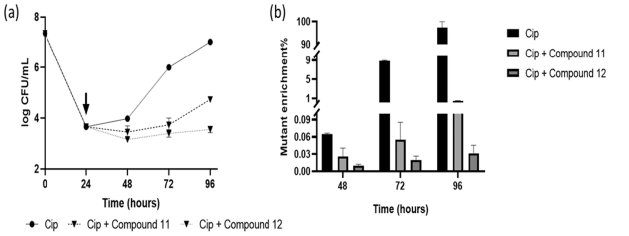

Figure 5. *M. smegmatis* delayed addition time-kill kinetics profile. (a) Reduction in the regrowth of ciprofloxacin (0.75 μg mL^{-1}) treated tolerant cells in the presence of compounds **11** and **12** (400 μg mL^{-1}); (b) reduction of resistant mutant generation during ciprofloxacin (0.75 μg mL^{-1}) treatment in the presence of **11** and **12** (400 μg mL^{-1}). Black arrows depict the time of compound addition.

the cells without isotetrones grew exponentially and reached to a cell population comparable to the time when drug treatment was initiated. Whereas, in the presence of derivatives **11** and **12**, regrowth was prevented remarkably up to 72 h. Studies earlier reported on varied bacteria pointed out how persister cells could act as the predecessor of resistant mutants.[66,67] In our assay since antibiotic-survived cells were able to grow in the presence of the same drug (ciprofloxacin), the possibility of emergence of resistant genetic mutants (cipro^{R}) was estimated by plating parallelly in ciprofloxacin containing MB plates. A visible increase in cipro^{R} mutants was observed during the plateau/nongrowing phase and, in the presence of isotetrones, a significant arrest of mutant enrichment occurred further. In the absence of isotetrones, namely, only in the presence of the drug, uninhibited resistant mutant enrichment over time occurred, with a remarkable ∼98% mutant population taking over within 48 h of the regrowth phase. Additionally, by patching individual colonies in a 5X ciprofloxacin plate at 96 h, we confirmed 100% of them are ciprofloxacin-resistant mutants (Figure S17). Both derivatives **11** and **12** significantly restricted resistant mutant enrichment for 48 h, presumably due to their inherent ability to slow regrowth of persisters and the subsequent transformation into mutants (Figure 5b). Our data further suggested that the nongrowing phase/plateau between 24 and 48 h in the assay is responsible for conversion of persisters into genetic mutants and this critical step could be successfully prevented by isotetrones. These observations tempt us to raise and prove that isotetrones **11** and **12**, in combination with ciprofloxacin, act as bioenhancers and are therapeutically superior when administered together. The combination significantly inhibited regrowth of drug-tolerant population and arrested the resistant mutant enrichment. These findings implicate in the larger context of preventing resistance to antibiotics.

Experiments of kill kinetics, regrowth assay, and mutant enrichment assays were performed with ciprofloxacin + vitamin C (4 mM, MIC concentration) and ciprofloxacin + derivative **12** (400 μg mL^{-1}). The experiments showed that the combination of ciprofloxacin (0.75 μg mL^{-1}) + vitamin C (4 mM) did not show any altered kill kinetics (Figure S15) and was unable to inhibit the regrowth of the drug-tolerant population over 72 and 96 h time points (Figure S18a). Furthermore, the ciprofloxacin + vitamin C combination did not arrest the resistant mutant enrichment at 72 and 96 h (Figure S18b). At 96 h, although the combination appeared more efficacious, as compared to ciprofloxacin alone, still the mutant enrichment percentage was significantly high, as compared to the ciprofloxacin + derivative **12** combinations. The result suggests that the inhibition of regrowth of ciprofloxacin survived population and mutant enrichment at a lower concentration of the drug is only possible in the presence of selective isotetrone derivatives and not in the presence of vitamin C alone. In all the kill kinetics and mutant detection assays, the initial inoculum was adjusted to ∼1 × 10^{7} CFU/mL, which is based on the ciprofloxacin resistance frequency value of *M. smegmatis* WT, i.e., 4.5 × 10^{-8},[63] to avoid any spontaneous mutant in the beginning of the assay.

Isotetrone 12 Kills Cells under Stringent Conditions. In order to verify whether isotetrones would affect the survival kinetics under PBS starvation, cells in the PBS solution were incubated with the derivatives, at 400 μg mL^{-1} f.c., and CFU was estimated after 72 h for 2 weeks. The derivative **12** was able to inactivate cells under PBS starvation in PBS (Figure 6).

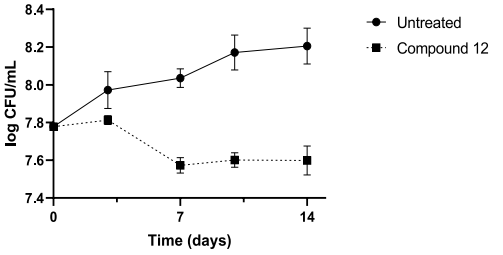

Figure 6. Plots of inhibition under long-term starvation of *M. smegmatis* in PBS (untreated) and in the presence of compound **12**.

The long-term survival in PBS-starved conditions is linked to (p)ppGpp stress alarmone proliferation and earlier studies showed that vitamin C interfered with (p)ppGpp biosynthesis.[64,65] in *M. smegmatis*. Isotetrones **12** might possibly interfere with the stress alarmone biosynthesis similarly, and thus, a visible drop in CFU was observed even in the absence of an antibiotic under such stringent conditions. There are previous reports of vitamin C interacting with Rel$_{Msm}$ enzyme[65] and since our result also indicated a possible role of isotetrone **12** in regulating stringent response in *M. smegmatis*, we checked the possible interaction of compound **12** with Rel$_{Msm}$ with molecular simulations.

Molecular Dynamics Simulation Reveals Notable Interactions between Compound 11, 12, and Rel$_{Msm}$. A systematic, molecular dynamics (MD) simulation study was undertaken to assess the binding interaction of the isotetrone derivative **12** and **11** with the Rel$_{Msm}$ enzyme, with the knowledge that vitamin C binds directly to Rel$_{Msm}$ enzyme and inhibits (p)ppGpp biosynthesis. Figure 7 shows the Rel$_{Msm}$−

https://doi.org/10.1021/acsomega.3c00822
ACS Omega 2023, 8, 20513−20523

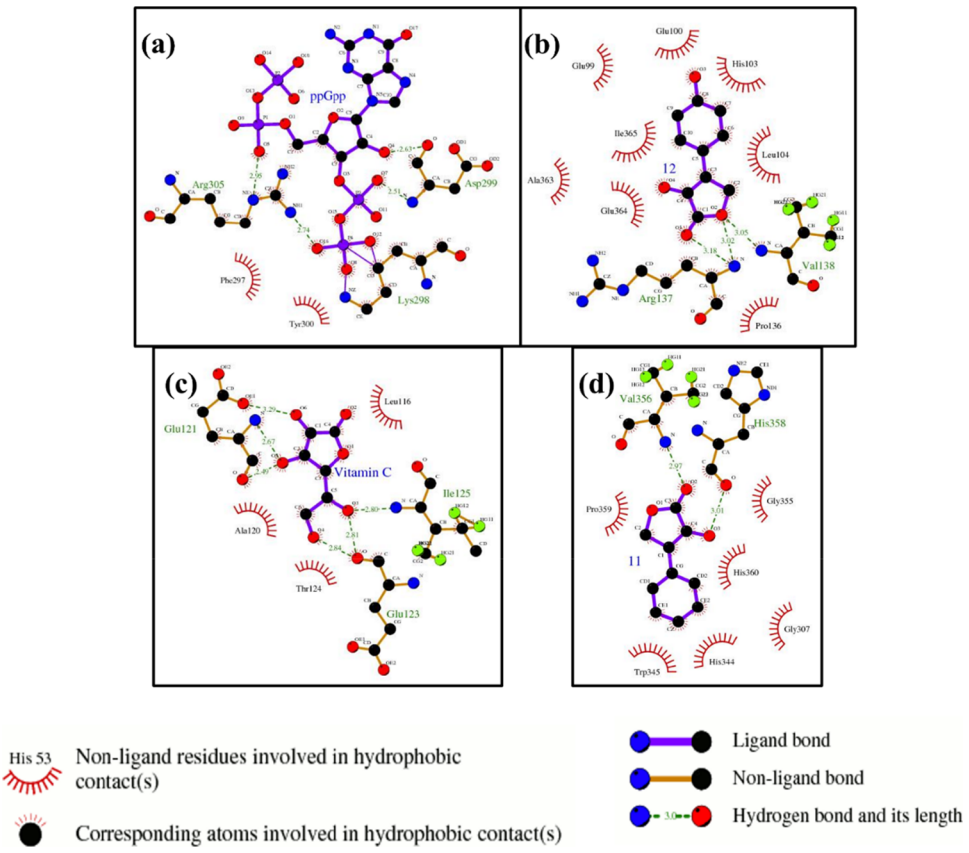

Figure 7. 2D interaction plots of various protein−ligand complexes, obtained from docking studies. (a) Rel_{Msm}-ppGpp; (b) Rel_{Msm}-derivative **12**; (c) Rel_{Msm}-vitamin C; and (d) Rel_{Msm}-derivative **11** complexes at their lowest energy conformations, predicted by molecular docking.

ligand complex at their most energetically preferable binding sites, found from the docking study. The corresponding binding affinity is tabulated in Table 1. The structures served as initial configurations for subsequent MD simulation study. The protein−ligand complex structures after 10 ns of simulation are depicted in Figure 8. It should be noted that we run short 10 ns long MD simulation to get the most realistic binding site before calculating binding energy. The binding sites obtained in the docking study are preserved during the MD simulation. The average binding energies (ΔH_{bind}) for ppGpp, compound **11**, **12**, and vitamin C, obtained from the simulated trajectories, are presented in Table 1. It is evident that ppGpp binds to Rel_{Msm} protein most strongly, followed by compound **12**, vitamin C, and compound **11**. In fact, compound **11** detached from the Rel_{Msm} at the end of the simulation (Figure 8d). The binding energy trend is mostly in agreement with the docking results. Figure 9a presents the contributions of electrostatic and VdW

Table 1. Binding Affinity Obtained from the Docking Study and Average Binding Energy as Calculated from MD-Simulated Trajectories Using MM-GBSA

ligand	ΔH (kcal/mol) from docking	ΔH (kcal/mol) from MM-GBSA
ppGpp	−8.17 ± 0.33	−38.58 ± 8.40
compound **12**	−4.66 ± 0.34	−9.74 ± 3.37
vitamin C	−3.35 ± 0.33	−4.01 ± 4.04
compound **11**	−4.36 ± 0.18	−3.88 ± 4.20

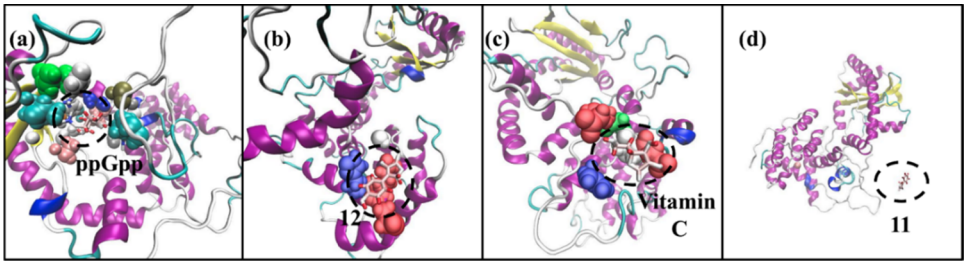

Figure 8. (a) Rel_{Msm}-ppGpp, (b) Rel_{Msm}-**12**, (c) Rel_{Msm}-vitamin C, and (d) Rel_{Msm}-**11** complexes after 10 ns simulation. The secondary structure of the protein has been represented with the color code: yellow: β sheet, pale blue: turns, and white: other residues. The ligands are presented using "licorice" representation scheme of VMD. Protein residues within a 5 Å distance from the ligands are presented using VdW spheres with a color code: White: nonpolar residues, blue: basic residues, red: acidic residues, and green: polar residues. Water molecules are removed for clarity.

https://doi.org/10.1021/acsomega.3c00822
ACS Omega 2023, 8, 20513−20523

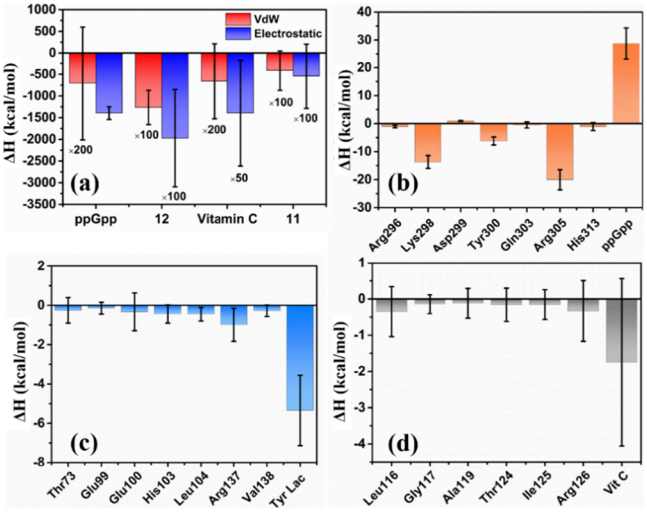

Figure 9. (a) Average electrostatic and VdW components of binding energy. Contribution of different residues in the binding energy for (b) Rel_{Msm}-ppGpp, (c) Rel_{Msm}-compound **12**, and (d) Rel_{Msm}-vitamin C complexes. Nomenclature: Tyr Lac: compound **12**; Vit C: vitamin C.

components of the binding energy, for all the four ligands. For ppGpp, it can be easily seen that the protein−ligand binding is mostly driven by the electrostatic energy, whereas the contribution from the VdW interaction is not significant (Figure 9a). This can be attributed to the presence of the phosphate groups on the ppGpp molecule. In the case of compound **12** and **11**, both the VdW and electrostatic energies significantly promoted the binding process (Figure 9a). Like ppGpp, vitamin C also binds to Rel_{Msm} through Coulombic interactions only, although the magnitude of the interaction was much smaller than the former (Figure 9a) because of the absence of any charged functional groups. An interesting observation is that in case of vitamin C, the electrostatic contribution to ΔH is higher than that of compound **12** (Figure 9a). Despite that, the binding affinity of vitamin C and Rel_{Msm} is weak, probably because of its higher solubility than compound **12**. It is noteworthy that not all the residues of the Rel protein took part in the ligand binding phenomena. The per residue decomposition data of ΔG_{bind} are depicted in Figure 9b−d. In corroboration with the previous observations, the significant contribution toward Rel_{Msm}-ppGpp binding came from the positively charged residues like Arg and Lys (Figure 9b). This is another evidence that the binding of ppGpp with Rel_{Msm} is dominated by the electrostatic interaction among the negatively charged phosphate groups present in ppGpp and the positively charged residues of the Rel_{Msm}. An interesting observation is that the contribution from ppGpp do not favor the protein−ligand binding (Figure 9b) due to a high positive change in the polar solvation energy upon binding (1364.06 ± 140.56 kcal/mol) to Rel, indicating the presence of an attractive Coulombic interaction between ppGpp and solvent molecules. For derivative **12** and vitamin C, no specific protein residues provided a major contribution toward the binding energy, rather significant contribution came from the ligands (Figure 9c,d). The absence of a charged group in **12** and vitamin C can be attributed as the probable reason behind this striking difference. A similar decomposition study was not performed on derivative **11**, due to very weak binding.

Apart from the electrostatic and VdW interactions, protein−ligand binding can also be mediated by the formation of hydrogen bonds (H-bonds) between the protein and ligand. We used a cutoff distance of 0.35 nm between donor−acceptor and a cutoff angle of 30° to define H-bonds. In the case of ppGpp and Rel_{Msm}, Lys298, Tyr300, and Arg305 residues were involved in H-bonding. For derivative **12**, Glu100, His103, Arg137residues, and for vitamin C, Leu116, and Arg126 residues were found to form H-bonds with ligands. The average number of hydrogen bonds formed between ppGpp and Rel_{Msm} was found to be the highest (9.23 ± 1.68), followed by **12** (1.18 ± 0.85) and vitamin C (1.31 ± 1.24). This occurred due to the presence of more H-bond forming acceptors and donors in ppGpp, compared to derivative **12** or vitamin C. On the other hand, derivative **11** hardly formed any H-bonds (0.36 ± 0.51) with Rel_{Msm} protein. Our simulation study confirms the experimental observation of the highest binding affinity of ppGpp, followed by derivative **12** and vitamin C. The highest binding energy of ppGpp is attributed to the presence of the phosphate group and also to its ability to form more hydrogen bonds with Rel_{Msm}.

The maximum concentration tested for the isotertrones **10**−**12** against *M. smegmatis* is ∼2 mM in the present work. The isotetrone derivatives possess an isomeric scaffold of the tetrone, to which vitamin C belongs to. Vitamin C was demonstrated to have inhibition efficacy against mycobacteria at a concentration of 10 mM.[58] The MIC values of vitamin C against *M. smegmatis* and *M. tuberculosis* are 8 and 1 mM, respectively.[18] Vitamin C also possesses a bactericidal activity at 4 mM. Furthermore, the synthetic isotetrones are studied in the present study as adjuvants in order to enhance the inhibition efficacies of ciprofloxacin, by preventing the persister cell regrowth and mutant enrichment. Such an effect would not arise by monotherapy. In a related study involving acute and chronic infection models of *M. tuberculosis* in mice,[68] it was shown that vitamin C at 1 mM concentration, in combination with rifampicin and isoniazid, potentiates in vivo killing by 1 log and that optimum concentration in serum can be achieved by i.p. infection.[68] It is noted that vitamin C is a part of regular diet, and high doses of vitamin C stands to be safe[69] to achieve a human plasma concentration of up to 49 mM.[70,71] Considering the above aspects on tetrone scaffolds, we adjudge that the isotetrones studied herein, ∼200 and 400 μg mL^{-1} concentrations, are relatively lower and better when compared to vitamin C as inhibitors of not only the planktonic growth but also stationary phase processes. Combined with lesser cytotoxicities, these derivatives show a promise as scaffolds for inhibitor development for mycobacterial persister cells.

The present investigation focuses on advancing the scaffold, namely, tetrone and isotetrone in mycobacterium growth and stationary phase processes. The work follows the results on vitamin C, which was demonstrated earlier to possess inhibition activities for the above processes. The tetrone scaffold of vitamin C prompted us to investigate the isomeric isotetrone scaffold. The synthetic method was thus developed to prepare a number of isotetrones, each one differing at the substituent nature at the *C*-4 carbon of the scaffold. The variation in the substituent was chosen such that aliphatic and aromatic substituents were covered. Within these substitutions, functionalities were varied, so as to present the phenolic moiety, indole moiety, and phenyl moiety as the substituent in one series. In another series, methyl, ethyl, and isopropyl substituents in a quaternary carbon were prepared. The

https://doi.org/10.1021/acsomega.3c00822
ACS Omega 2023, 8, 20513−20523

isotetrone further was presented either in a keto or enol or a hydroxy functionality at the *C*-3 carbon. These variations are representatives of different series that are functionalized on the scaffold. The focus was to identify the functionalities on the scaffold that would show promise for further involved biological and computational studies. These studies require the scaffold functionality that exhibits the most effect. As detailed above, the present scaffold functionalization search is covered with complementarity in the nature of functionalization. Aryl substituents at *C*-4 carbon in derivatives **11** and **12** show the most efficacy in both mycobacterial growth, biofilm inhibition, and inhibition of persister cells in combination therapy, as observed in this study. Derivatives **13**−**15** also did not exhibit effects neither on growth nor biofilm inhibitions. Results from these sets of derivatives provide a clue for further advancement, where the direct attachment of the aryl moiety on the tetrone scaffold would be the focus for further inhibitor diversification and SAR studies.

CONCLUSIONS

The work herein demonstrates (i) chemical synthesis of hitherto unknown *C*-4 modified isotetrones from α-amino acids, through the formation of pyruvic acids, their aldonization, and lactonization. (ii) Biochemical studies discover the role of these new isotetrones to interfere the growth of mycobacterium planktonic cells; inhibition of *M. smegmatis* biofilm formation is seen in a dose-dependent manner. (iii) Synergistic inhibitory effects are observed with well-known antibiotic ciprofloxacin in the presence of the selected isotetronic acids, wherein the MIC of ciprofloxacin is improved by twofold. (iv) Specific activities of isotetrones possessing aromatic substituents at *C*-4 carbon include the prevention of the regrowth of antibiotic-tolerant population in *M. smegmatis*. We observe that *M. smegmatis* cells survive without isotetrones, form nongrowing persisters, and resuscitate in the presence of lower concentrations of antibiotic ciprofloxacin, presumably due to enrichment of genetic mutants as it occurs in a clinical scenario. (v) Systematic MD simulations uncover the stabilities of Rel_{Msm} protein−inhibitor complexes, occurring through VdW, electrostatic, and hydrogen-bonding interactions. The study shows that the addition of isotetrones hamper the regrowth stage of ciprofloxacin-selected persister population. Recurrent infection is a challenge in current antibiotic treatment regimens. The present work demonstrates the complete occlusion of the generation of resistant mutants, thereby opening up the feasibility to administer fewer concentrations of antibiotics and minimize associated off-target effects.

EXPERIMENTAL SECTION

General Procedure. Formalin and K_2CO_3 were sequentially added to the solution of keto acid, derived from L-valine, L-leucine, L-isoleucine, *L*-phenylalanine, L-tyrosine, and L-tryptophan in THF, and stirred at room temperature for 3−15 h. The solution was evaporated in vacuo, and the reaction mixture was treated with aq. HCl (3 N), extracted with Et_2O (3 × 15 mL), organic portion washed with water (10 mL), brine (10 mL), and dried over Na_2SO_4 and concentrated in vacuo.

*3-Hydroxy-4-isopropylfuran-2(5H)-one (**10**).* Formalin (0.38 mL, 4.62 mmol) and K_2CO_3 (0.66 g, 4.84 mmol) were sequentially added to a stirred solution of **7**[53] (0.5 g, 3.85 mmol) in THF (5 mL), stirred for 4 h at room temperature, and worked up as described in the general procedure. The crude product was purified by column chromatography (SiO_2) (pet. Ether/EtOAc, linear gradient) to afford **10** (0.12 g, 34%) as a colorless oil. R_f (pet. Ether/EtOAc = 7:3) 0.4. ^{1}H NMR ($CDCl_3$, 400 MHz): δ 4.68 (s, 2 H, CH_2O), 2.89 (m, 1 H, $CH(CH_3)_2$), 1.18 (d, J = 6.8 Hz, 6 H, $CH(CH_3)_2$); ^{13}C NMR ($CDCl_3$, 100 MHz): δ 171.7, 137.5, 135.6, 68.1, 25.5, 20.4. GCMS: *m*/*z* calcd. For $C_7H_{10}O_3$: 142 [M+], found 142, with fragments at *m*/*z* at 97, 69 and 41.

*3-Hydroxy-4-phenylfuran-2(5H)-one (**11**).* Formalin (0.09 mL, 1.08 mmol) and K_2CO_3 (0.14 g, 1.14 mmol) were added sequentially to a solution of **8**[54] (0.15 g, 0.9 mmol) in THF (2.5 mL), and the reaction mixture was stirred for 4 h at room temperature and worked up as described in the general procedure. The residue was purified by column chromatography (SiO_2) (pet. ether/EtOAc, linear gradient) to afford **11** (0.073 g, 56%) as a white solid. Mp 135.8 °C. R_f (pet. ether/EtOAc = 9:1) 0.7. ^{1}H NMR (CD_3OD, 400 MHz): δ 7.66 (d, J = 8 Hz, 2 H, C_6H_5), 7.36 (t, J = 8 Hz, 2 H, C_6H_5), 7.29−7.26 (m, 1 H, C_6H_5), 5.03 (s, 2H, CH_2O); ^{13}C NMR (CD_3OD, 400 MHz): δ 172.3, 138.8, 134.01, 132.2, 130.7, 129.9, 129.7, 129.4, 127.6, 69.2. HRMS: m/z calcd. For $C_{10}H_8O_3$: 177.0552 $[M + H]^+$, found 177.0551.

*3-Hydroxy-4-(4-hydroxyphenyl)furan-2(5H)-one (**12**).* Formalin (0.16 mL, 1.94 mmol) and K_2CO_3 (0.28 g, 2.04 mmol) were successively added to a solution of **9**[54] (0.35 g, 1.94 mmol) in THF (5 mL), stirred for 4 h at room temperature, and worked up as described in the general procedure. Column chromatography (SiO_2) (pet. ether/EtOAc, linear gradient) of the residue afforded **12** (0.127 g, 47%) as a white solid. Mp 144.9 °C. R_f (pet. ether/EtOAc = 3:2) 0.5. ^{1}H NMR (CD_3OD, 400 MHz): δ 7.59 (d, J = 8.8 Hz, 2 H, C_6H_5), 6.83 (d, J = 8.4 Hz, 2 H, C_6H_5), 5.06 (s, 2 H, CH_2O); ^{13}C NMR (CD_3OD, 100 MHz): δ 172.8, 159.6, 136.5, 129.3, 128.8, 123.6, 116.6, 69.2. HRMS: m/z calcd. For $C_{10}H_9O_4$: 193.0501 $[M + H]^+$, found 193.0501.

*3-Hydroxy-4,4-dimethyldihydrofuran-2-one (**13**).* Formalin (1.75 mL, 21.5 mmol) and K_2CO_3 (1.5 g, 10.75 mmol) were added successively to a solution of 2-oxoisovaleric acid[55] (0.5 g, 4.3 mmol) in THF (5 mL); the reaction was stirred for 15 h at room temperature and worked up as described in the general procedure. Vacuum distillation was performed to remove the unreacted starting material and column chromatography (SiO_2) (pet. ether/EtOAc, linear gradient) of the residue gave **13** (0.19 g, 34%) as a solid. Mp 84.3 ± 2 °C. R_f (pet. ether/EtOAc = 9:1) 0.8. ^{1}H NMR ($CDCl_3$, 400 MHz): δ 4.15 (s, 1 H, CHOH), 3.98 (d, J = 9.2 Hz, 1 H, CH_2O), 3.92 (d, J = 9.2 Hz, 1 H, CH_2O), 1.18 (s, 3 H, CH_3), 1.03 (s, 3 H, CH_3); ^{13}C NMR ($CDCl_3$, 100 MHz): δ 178.1, 76.4, 75.6, 40.7, 22.6, 18.7. GC−MS: *m*/*z* calcd. For $C_6H_{10}O_3$: 131 [M + H], found 131, with fragments at *m*/*z* at 71, 57, 43 and 41.

*4-Ethyl-4-methyl-dihydrofuran-2,3-dione (**14**).* Formalin (1.9 mL, 23.1 mmol) and K_2CO_3 (1.6 g, 11.55 mmol) were added successively to a solution of 3-methyl-2-oxopentanoic acid[57] (0.5 g, 3.85 mmol) in THF (5 mL), stirred for 15 h, and worked up as described in the general procedure. The residue was purified by vacuum distillation to afford **14** (0.29 g, 54%) as a yellow liquid. (R_f) (pet. ether/EtOAc = 9:1) 0.8. ^{1}H NMR ($CDCl_3$, 400 MHz): δ 4.55 (d, J = 9.6 Hz, 1 H, CH_2O), 4.39 (d, J = 9.6 Hz, 1 H, CH_2O), 1.78−1.62 (m, 2 H, CH_2CH_3), 1.26 (s, 3 H, CH_3), 0.92 (t, J = 7.2 Hz, 3 H, CH_2CH_3); ^{13}C NMR ($CDCl_3$, 100 MHz): δ 198.4, 161, 75.6, 45.4, 29.3, 19.4,

https://doi.org/10.1021/acsomega.3c00822
ACS Omega 2023, 8, 20513−20523

8.10. GCMS: *m/z* calcd. For $C_7H_{10}O_3$: 142 [M+], found 142, with fragments at *m/z* at 85, 71, 69, 55 and 41.

*3-Hydroxy-4-(1-hydroxymethyl)-1H-indol-3-yl)furan-2(5H)-one (**15**).* Formalin (0.22 mL, 2.71 mmol) and K_2CO_3 (0.38 g, 2.71 mmol) were added successively to a solution of indole-3-pyruvic acid[56] (0.5 g, 2.46 mmol) in THF (5 mL) was treated with, and the reaction was stirred for 6 h at room temperature and worked up as described in the general procedure. The crude product was purified by column chromatography (SiO_2) (pet. ether/EtOAc, linear gradient) to afford **15** (0.174 g, 33%) as a white solid. Mp 113.4 ± 2 °C. R_f (pet. ether/EtOAc = 3:1) 0.3. ^{1}H NMR (CD_3OD, 400 MHz): δ 7.96 (s, 1 H, C*H*NH), 7.82 (d, J = 8 Hz, 1 H, C_6H_5), 7.59 (d, J = 8 Hz, 1 H, C_6H_5), 7.28 (t, J = 8 Hz, 1 H, C_6H_5), 7.19 (t, J = 8 Hz, 1 H, C_6H_5), 5.63 (s, 2 H, CH_2O), 5.29 (s, 2 H, CH_2O); ^{13}C NMR (CD_3OD, 100 MHz): δ 171.2, 136.1, 133.1, 129.2, 126.4, 126.2, 122.3, 120.7, 120.5, 110.1, 107, 69, 68.1. HRMS: m/z calcd. For $C_{13}H_{11}NO_4$: 246.0766 $[M + H]^+$, found 246.0767.

Bacterial Growth and Culture Conditions. For all the assays, the *M. smegmatis* mc^{2}155 strain was grown in MB7H9 media (HiMedia) containing 0.05% Tween-80 and 2% glucose; agar (1.6%, w/v) (Himedia) was used to make agar plates. Ciprofloxacin powder was obtained from Sisco Research Laboratories. Antibiotics were used at variable concentrations. Unless mentioned otherwise, strains were grown at 37 °C and 150 rpm.

Growth Inhibition Assay. For analyzing the effect of isotetrones on the growth of the *M. smegmatis* mc^{2}155 strain, bacteria were grown till the mid-exponential phase, further inoculation was done in MB7H9 media containing 0.05% Tween-80 and 2% glucose to make the final OD ∼ 0.03. Such culture (3 mL) was taken in a sterile glass tube, and 30 μL of each of the respective isotetrones with varying final concentrations (100, 200, 300, and 400 μg mL^{-1}) was added to the media at 0 h, and OD_{600} nm was measured. The bacterial growth was further monitored in equal intervals for 96 h by recording OD_{600} and plotted using Graph Pad Prism Software. The tube containing no compounds (only DMSO) served as the untreated positive control to observe and compare growth inhibition in the presence and absence of the compounds. This experiment was performed in a set of two experimental replicates.

Biofilm Formation Assay. The primary culture for the wild-type strain *M. smegmatis* mc^2 155 was grown in MB7H9 medium at 37 °C, 150 rpm shaking. The cells were harvested at the stationary phase and washed with Sauton's media (Himedia) twice, the cell pellet was resuspended in the Sauton's media containing 2% glucose, and the final OD was adjusted to 0.05. Subsequently, 200 μL of culture was poured into a well of sterile 96-well microtiter plates supplemented with 2 μL respective isotetrones having a final concentration of 100, 200, 300, and 400 μg mL^{-1}. The control wells included in the same plate were untreated control (only cells, no compounds to monitor uninhibited biofilm formation) and media control (only media, no cells to monitor contamination). The inoculated plates were sealed and kept in a 37 °C humidified incubator to avoid drying of media and incubated for a minimum of 72−96 h without external disturbance. The images were captured under white light at different time points. The experiment was performed in a set of three biological replicates.

MIC Determination. For analyzing if the isotetrones could increase the susceptibility to ciprofloxacin, we performed an MIC assay using the ciprofloxacin in combination with compounds (200 μg mL^{-1} f.c.) by broth microdilution assay using resazurin dye. Ciprofloxacin was 2-fold diluted in the 96-well microplate to achieve a broad range of final concentrations ranging from 16 to 0.03 μg mL^{-1}. *M. smegmatis* cultures were grown till mid-exponential phase (OD_{600} of 0.6−1), diluted to OD_{600} of 0.01 in fresh MB7H9 medium, and 196 μL was added in each well of the 96-well plate containing 4 μL of different concentrations of ciprofloxacin. Depending on the series, cells were premixed with different isotetrones (200 μg mL^{-1} f.c.); in the no-compound series, an equal amount of sterile miliQ was added. Following the incubation of 36 h standing at 37 °C, 30 μL of 0.1 mg mL^{-1} of resazurin was added to each of the wells and again incubated for 6−8 h at 37 °C, and the dye reduction value was recorded.

Time-Kill Kinetics Assay. *M. smegmatis* cultures were grown till the late exponential/stationary phase (OD_{600} of 1.5−2.5), diluted 1:100 to start a secondary culture and grown till the mid-exponential phase (OD_{600} of 0.6−1), and further diluted to adjust to OD_{600} of 0.2 corresponding to ∼2 × 10^7 CFU mL^{-1} (CFU = colony-forming unit) in the fresh MB7H9 medium. The culture (3 mL) was added to a tube and 2.5 μg mL^{-1} (f.c.) ciprofloxacin (10X MIC) was added with or without isotetrones (400 μg mL^{-1}) at T-0, and CFU mL^{-1} was estimated by spreading into the MB7H9 agar plate. Tubes were incubated at 37 °C in a shaker, and CFU estimations (plating) were done every 24 h up to 96 h. Plates were further incubated at 37 °C for 3−4 days for colony growth and subsequently counted. In order to measure the killing efficiency of the compounds alone (without ciprofloxacin), a similar kill kinetics assay was set up in parallel. All kill kinetics assays were performed with at least 3 biological replicates.

Delayed Addition of Isotetrones in Time-Kill Kinetics. *M. smegmatis*. Secondary culture was prepared as mentioned above, and then, 0.75 μg mL^{-1} of ciprofloxacin (3X MIC) was added to the media. After 24 h of incubation, the culture was divided into separate tubes and different isotetrones were added (400 μg mL^{-1} f.c.). CFU estimations (plating) were performed every 24 h up to 96 h. The tube containing no compounds (only DMSO) served as the untreated control to compare regrowth in the absence of the compounds. This experiment was performed in a set of three replicates.

Mutant Enrichment Determination. In parallel to the CFU estimation in kill kinetics, spotting/spreading was conducted in ciprofloxacin (1.25 μg mL^{-1}) plates to enumerate resistant mutant population enrichment over time.

Kill Kinetics under Nutrient Starvation. *M. smegmatis* cultures were grown till the late exponential/stationary phase (OD_{600} of 1.5−2.5), diluted 1:100 to start a secondary culture, and grown till the mid-exponential phase (OD_{600} of 0.6−1). After that, the cells were washed twice with PBS and resuspended in an equal volume of PBS. T-0 CFU mL^{-1} estimation was done immediately, and the culture was divided into equal volumes in several glass tubes followed by the addition of selective isotetrones (400 μg mL^{-1} f.c.). In the untreated control tube, an equal volume of sterile MilliQ water was added. CFU estimation was done every 72 h for ∼3 weeks.

https://doi.org/10.1021/acsomega.3c00822
ACS Omega 2023, 8, 20513−20523

■ ASSOCIATED CONTENT

Supporting Information

The Supporting Information is available free of charge at https://pubs.acs.org/doi/10.1021/acsomega.3c00822.

Docking and molecular dynamics simulation protocol; NMR spectra of new compounds; and kill kinetics and persister regrowth (PDF)

■ AUTHOR INFORMATION

Corresponding Authors

Prabal Kumar Maiti − *Department of Physics, Indian Institute of Science, Bangalore 560 012, India*; orcid.org/0000-0002-9956-1136; Email: maiti@iisc.ac.in

Anirban Ghosh − *Molecular Biophysics Unit, Indian Institute of Science, Bangalore 560 012, India*; Email: ganirban@iisc.ac.in

Narayanaswamy Jayaraman − *Department of Organic Chemistry, Indian Institute of Science, Bangalore 560 012, India*; orcid.org/0000-0001-5577-8053; Email: jayaraman@iisc.ac.in

Authors

Kingshuk Bag − *Department of Organic Chemistry, Indian Institute of Science, Bangalore 560 012, India*

Aditya Kumar Pal − *Molecular Biophysics Unit, Indian Institute of Science, Bangalore 560 012, India*; orcid.org/0000-0003-3005-7668

Subhadip Basu − *Department of Physics, Indian Institute of Science, Bangalore 560 012, India*

Mamta Singla − *Molecular Biophysics Unit, Indian Institute of Science, Bangalore 560 012, India*

Biplab Sarkar − *Molecular Biophysics Unit, Indian Institute of Science, Bangalore 560 012, India*

Dipankar Chatterji − *Molecular Biophysics Unit, Indian Institute of Science, Bangalore 560 012, India*; orcid.org/0000-0002-9985-0632

Complete contact information is available at: https://pubs.acs.org/10.1021/acsomega.3c00822

Author Contributions

D.C., P.M., A.G. and N.J. contributed to the conception and design of the study. K.B., A.P., S.B. M.S. and A.G. performed the experiments. D.C., P.M., A.G. and N.J. participated in data analysis and interpretation. All authors participated in writing the manuscript.

Notes

The authors declare no competing financial interest.

■ ACKNOWLEDGMENTS

The authors thank the Department of Biotechnology (DBT), Government of India, for funding this work (Grant number: BT/PR33123/MED/29/1497/2020). Indian Institute of Science, Bangalore, is gratefully acknowledged for a research fellowship to K.B.

■ REFERENCES

(1) Harms, A.; Maisonneuve, E.; Gerdes, K. Mechanisms of Bacterial Persistence During Stress and Antibiotic Exposure. *Science* **2016**, *354*, No. aaf4268.

(2) Chatterji, D.; Ojha, A. K. Revisiting the Stringent Response, ppGpp And Starvation Signaling. *Curr. Opin. Microbiol.* **2001**, *4*, 160−165.

(3) Srivatsan, A.; Wang, J. D. Control of Bacterial Transcription, Translation and Replication by (p)ppGpp. *Curr. Opin. Microbiol.* **2008**, *11*, 100−105.

(4) Hengge, R. High-Specificity Local and Global c-di-GMP Signaling. *Trends Microbiol.* **2021**, *29*, 993−1003.

(5) Kushwaha, G. S.; Oyeyemi, B. F.; Bhavesh, N. S. Stringent Response Protein as A Potential Target to Intervene Persistent Bacterial Infection. *Biochimie* **2019**, *165*, 67−75.

(6) Sharma, I. M.; Petchiappan, A.; Chatterji, D. Quorum Sensing and Biofilm Formation in Mycobacteria: Role of c-di-GMP and Methods to Study This Second Messenger. *IUBMB Life* **2014**, *66*, 823−834.

(7) Hogg, T.; Mechold, U.; Malke, H.; Cashel, M.; Hilgenfeld, R. Conformational Antagonism Between Opposing Active Sites in A Bifunctional RelA/SpoT Homolog Modulates (p)ppGpp Metabolism During the Stringent Response [corrected]. *Cell* **2004**, *117*, 57−68.

(8) Page, R.; Peti, W. Toxin-Antitoxin Systems in Bacterial Growth Arrest and Persistence. *Nat. Chem. Biol.* **2016**, *12*, 208−214.

(9) Syal, K.; Joshi, H.; Chatterji, D.; Jain, V. Novel pppGpp Binding Site at the C-Terminal Region of the Rel Enzyme from *Mycobacterium smegmatis*. *FEBS J.* **2015**, *282*, 3773−3785.

(10) Liu, S.; Wu, N.; Zhang, S. S.; Yuan, Y. H.; Zhang, W. H.; Zhang, Y. Variable Persister Gene Interactions with (p)ppgpp for Persister Formation in *Escherichia coli*. *Front Microbiol.* **2017**, *8*, 1795.

(11) Tian, C.; Semsey, S.; Mitarai, N. Synchronized Switching of Multiple Toxin−Antitoxin Modules by (p)ppGpp Fluctuation. *Nucleic Acids Res.* **2017**, *45*, 8180−8189.

(12) Petchiappan, A.; Chatterji, D. Antibiotic Resistance: Current Perspectives. *ACS Omega* **2017**, *2*, 7400−7409.

(13) Rhee, H. W.; Lee, C. R.; Cho, S. H.; Song, M. R.; Cashel, M.; Choy, H. E.; Seok, Y. J.; Hong, J. I. Selective Fluorescent Chemosensor for the Bacterial Alarmone (p)ppGpp. *J. Am. Chem. Soc.* **2008**, *130*, 784−785.

(14) Wexselblatt, E.; Kaspy, I.; Glaser, G.; Katzhendler, J.; Yavin, E. Design, Synthesis and Structure-Activity Relationship of Novel Relacin Analogs as Inhibitors of Rel Proteins. *Eur. J. Med. Chem.* **2013**, *70*, 497−504.

(15) Sureka, K.; Ghosh, B.; Dasgupta, A.; Basu, J.; Kundu, M.; Bose, I. Positive Feedback and Noise Activate the Stringent Response Regulator Rel in Mycobacteria. *PLoS One* **2008**, *3*, No. e1771.

(16) Syal, K.; Bhardwaj, N.; Chatterji, D. Vitamin C Targets (p)ppGpp Synthesis Leading to Stalling of Long-Term Survival and Biofilm Formation in *Mycobacterium smegmatis*. *FEMS Microbiol. Lett.* **2017**, *364*, No. fnw282.

(17) Vilchèze, C.; Kim, J.; Jacobs, W. R., Jr. Vitamin-C Potentiates the Killing of *Mycobacterium tuberculosis* by the First-Line Tuberculosis Drugs Isoniazid and Rifampin in Mice. *Antimicrob. Agents Chemother.* **2018**, *62*, No. e02165-17.

(18) Vilchèze, C.; Hartman, T.; Weinrick, B.; Jacobs, W. R., Jr. *Mycobacterium tuberculosis* is Extraordinarily Sensitive to Killing by A Vitamin C-Induced Fenton Reaction. *Nat. Commun.* **2013**, *4*, 1881.

(19) Keren, I.; Kaldalu, N.; Spoering, A.; Wang, Y.; Lewis, K. Persister Cells and Tolerance to Antimicrobials. *FEMS Microbiol. Lett.* **2004**, *230*, 13−18.

(20) Peddireddy, V.; Doddam, S. N.; Ahmed, N. Mycobacterial Dormancy Systems and Host Responses in Tuberculosis. *Front. Immunol.* **2017**, *8*, 84.

(21) Ranjitha, J.; Rajan, A.; Shankar, V. Features of the Biochemistry of *Mycobacterium smegmatis*, as a Possible Model for *Mycobacterium tuberculosis*. *J. Infect. Public Health* **2020**, *13*, 1255−1264.

(22) Princiotto, S.; Jayasinghe, L.; Dallavalle, S. Recent Advances in the Synthesis of Naturally Occurring Tetronic Acids. *Bioorg. Chem.* **2022**, *119*, No. 105552.

(23) Fischer, P. M.; Lane, D. P. Inhibitors of Cyclin-Dependent Kinases as Anti-Cancer Therapeutics. *Curr. Med. Chem.* **2000**, *7*, 1213−1245.

(24) Nishio, K.; Ishida, A.; Arioka, H.; Kurokawa, H.; Fukuoka, K.; Nomoto, T.; Fukumoto, H.; Yokote, H.; Saijo, N. Antitumor Effects

of Butyrolactone I, A Selective cdc2 Kinase Inhibitor, on Human Lung Cancer Cell Lines. *Anticancer Res.* **1996**, *16*, 3387−3395.
(25) Suzuki, M.; Hosaka, Y.; Matsushima, H.; Goto, T.; Kitamura, T.; Kawabe, K. Butyrolactone I Induces Cyclin B1 and Causes G2/M Arrest and Skipping of Mitosis in Human Prostate Cell Lines. *Cancer Lett.* **1999**, *138*, 121−130.
(26) Parvatkar, R. R.; D'Souza, C.; Tripathi, A.; Naik, C. G. Aspernolides A and B, Butenolides from A Marine-Derived Fungus *Aspergillus terreus*. *Phytochemistry* **2009**, *70*, 128−132.
(27) Haritakun, R.; Rachtawee, P.; Chanthaket, R.; Boonyuen, N.; Isaka, M. Butyrolactones from the Fungus *Aspergillus terreus* BCC 4651. *Chem. Pharm. Bull.* **2010**, *58*, 1545−1548.
(28) Adpressa, D. A.; Loesgen, S. Bioprospecting Chemical Diversity and Bioactivity in A Marine Derived *Aspergillus terreus*. *Chem. Biodiversity* **2016**, *13*, 253−259.
(29) Dewi, R. T.; Tachibana, S.; Darmawan, A. Effect On A-Glucosidase Inhibition and Antioxidant Activities of Butyrolactone Derivatives from *Aspergillus terreus* MC751. *Med. Chem. Res.* **2014**, *23*, 454−460.
(30) Niu, X.; Dahse, H. M.; Menzel, K. D.; Lozach, O.; Walther, G.; Meijer, J.; Grabley, S.; Sattler, I. Butyrolactone I Derivatives from *Aspergillus terreus* Carrying an Unusual Sulfate Moiety. *J. Nat. Prod.* **2008**, *71*, 689−692.
(31) Sugiyama, Y.; Yoshida, K.; Abe, N.; Hirota, A. Soybean Lipoxygenase Inhibitory and DPPH Radical-Scavenging Activities of Aspernolide A and Butyrolactones I and II. *Biosci., Biotechnol., Biochem.* **2010**, *74*, 881−883.
(32) Brachmann, A. O.; Forst, S.; Furgani, G. M.; Fodor, A.; Bode, H. B. Xenofuranones A and B: Phenylpyruvate Dimers from *Xenorhabdus szentirmaii*. *J. Nat. Prod.* **2006**, *69*, 1830−1832.
(33) Ingerl, A.; Justus, K.; Hellwig, V.; Steglich, W. Syntheses of Retipolide E and Ornatipolide, 14-Membered Biaryl-ether Macrolactones from Mushrooms. *Tetrahedron* **2007**, *63*, 6548−6557.
(34) Justus, K.; Herrmann, R.; Klamann, J.-D.; Gruber, G.; Hellwig, V.; Ingerl, A.; Polborn, K.; Steffan, B.; Steglich, W. Retipolides − Unusual Spiromacrolactones from the Mushrooms *Retiboletus retipes* and *R. ornatipes*. *Eur. J. Org. Chem.* **2007**, *2007*, 5560−5572.
(35) Nitta, K.; Fujita, N.; Yoshimura, T.; Arai, K.; Yamamoto, Y. Metabolic Products of *Aspergillus Terreus*. IX. Biosynthesis of Butyrolactone Derivatives Isolated from Strains IFO 8835 and 4100. *Chem. Pharm. Bull.* **1983**, *31*, 1528−1533.
(36) Machajewski, T. M.; Wong, C.-H. The Catalytic Asymmetric Aldol Reaction. *Angew. Chem., Int. Ed.* **2000**, *39*, 1352−1375.
(37) Allen, S. T.; Heintzelman, G. R.; Toone, E. J. Pyruvate Aldolases as Reagents for Stereospecific Aldol Condensation. *J. Org. Chem.* **1992**, *57*, 426−427.
(38) Enders, D.; Dyker, H.; Leusink, F. R. Enantioselective Synthesis of Protected Isotetronic Acids. *Chem. − Eur. J.* **1998**, *4*, 311−320.
(39) Dambruoso, P.; Massi, A.; Dondoni, A. Efficiency in Isotetronic Acid Synthesis Via A Diamine−acid Couple Catalyzed Ethyl Pyruvate Homoaldol Reaction. *Org. Lett.* **2005**, *7*, 4657−4660.
(40) Zhou, Z.; Walleser, P. M.; Tius, M. A. Isotetronic Acids from an Oxidative Cyclization. *Chem. Commun.* **2015**, *51*, 10858−10860.
(41) Mao, B.; Fañanas-Mastral, M.; Feringa, B. L. Catalytic Asymmetric Synthesis of Butenolides and Butyrolactones. *Chem. Rev.* **2017**, *117*, 10502−10566.
(42) Juhl, K.; Gathergood, N.; Jørgensen, K. A. Catalytic Asymmetric Homo-Aldol Reaction of Pyruvate-A Chiral Lewis Acid Catalyst that Mimics Aldolase Enzymes. *Chem. Commun.* **2000**, 2211−2212.
(43) Gathergood, N.; Juhl, K.; Poulsen, T. B.; Thordrup, K.; Jørgensen, K. A. Direct Catalytic Asymmetric Aldol Reactions of Pyruvates: Scope and Mechanism. *Org. Biomol. Chem.* **2004**, *2*, 1077−1085.
(44) Vincet, J. M.; Margottin, C.; Berlande, M.; Cavagnat, D.; Buffeteau, T.; Landais, Y. A Concise Organocatalytic and Enantioselective Synthesis of Isotetronic Acids. *Chem. Commun.* **2007**, 4782−4784.
(45) Roy, B.; Das, E.; Roy, A.; Mal, D. Ni(ii)-Catalyzed Vinylic C−H Functionalization of 2-Acetamido-3-Arylacrylates to Access Isotetronic Acids. *Org. Biomol. Chem.* **2020**, *18*, 3697−3706.
(46) Chen, P.; Wang, K.; Zhang, B.; Guo, W.; Liu, Y.; Li, C. Water Enables an Asymmetric Cross Reaction of α-Keto Acids With α-Keto Esters for the Synthesis of Quaternary Isotetronic Acids. *Chem. Commun.* **2019**, *55*, 12813−12816.
(47) Zhang, B.; Jiang, Z.; Zhou, X.; Lu, S.; Li, J.; Liu, Y.; Li, C. The Synthesis of Chiral Isotetronic Acids with Amphiphilic Imidazole/Pyrrolidine Catalysts Assembled in Oil-In-Water Emulsion Droplets. *Angew. Chem., Int. Ed.* **2012**, *51*, 13159−13162.
(48) Xu, X. -Y.; Tang, Z.; Wang, Y. -Z.; Luo, S. W.; Cun, L. F.; Gong, L. -Z. Asymmetric Organocatalytic Direct Aldol Reactions of Ketones with α-keto acids and their Application to the Synthesis of 2-Hydroxy-γ-Butyrolactones. *J. Org. Chem.* **2007**, *72*, 9905−9913.
(49) Lee, D.; Newman, S. G.; Taylor, M. S. Boron-Catalyzed Direct Aldol Reactions of Pyruvic Acids. *Org. Lett.* **2009**, *11*, 5486−5489.
(50) Cooper, A. J. L.; Ginos, J. Z.; Meister, A. Synthesis and Properties of the α-Keto Acids. *Chem. Rev.* **1983**, *83*, 321−358.
(51) Liu, Y.-X.; Zhang, P.-X.; Li, Y.-Q.; Song, H.-B.; Wang, Q.-M. Design, Synthesis, and Biological Evaluation Of 2-Benzylpyrroles and 2-Benzoylpyrroles Based on Structures of Insecticidal Chlorfenapyr and Natural Pyrrolomycins. *Mol. Diversity* **2014**, *18*, 593−598.
(52) Gräßle, S.; Vanderheiden, S.; Hodapp, P.; Bulat, B.; Nieger, M.; Jung, N.; Bräse, S. Solid Phase Synthesis of (Benzannelated) Six-Membered Heterocycles via Cyclative Cleavage of Resin-Bound Pseudo-Oxazolones. *Org. Lett.* **2016**, *18*, 3598−3601.
(53) Furukawa, K.; Inada, H.; Shibuya, M.; Yamamoto, Y. Chemoselective Conversion from α-Hydroxy Acids to α-Keto Acids Enabled by Nitroxyl-Radical-Catalyzed Aerobic Oxidation. *Org. Lett.* **2016**, *18*, 4230−4233.
(54) Yu, J.; Li, J.; Cao, S.; Wu, T.; Zeng, S.; Zhang, H.; Liu, J.; Jiao, Q. Chemoenzymatic Synthesis of L-3,4-Dimethoxyphenyl-Alanine and Its Analogues Using Aspartate Aminotransferase as A Key Catalyst. *Catal. Commun.* **2019**, *120*, 28−32.
(55) Endo, Y.; Shudo, K.; Itai, A.; Hasegawa, M.; Sakai, S. I. Synthesis and Stereochemistry of Indolactam-V, An Active Fragment of Teleocidins. Structural Requirements for Tumor-Promoting Activity. *Tetrahedron* **1986**, *42*, 5905−5924.
(56) Bergman, J.; Lidgren, G.; Gogoll, A. Synthesis and Reactions of Oxazolones from L-Tryptophan and α-Haloacetic Anhydrides. *Bull. Soc. Chim. Belg.* **1992**, *101*, 643−660.
(57) Lin, D. W.; Masuda, T.; Biskup, M. B.; Nelson, J. D.; Baran, P. S. Synthesis-Guided Structure Revision of the Sarcodonin, Sarcoviolin, and Hydnellin Natural Product Family. *J. Org. Chem.* **2011**, *76*, 1013−1030.
(58) Sikri, K.; Duggal, P.; Kumar, C.; Batra, S. D.; Vashist, A.; Bhaskar, A.; Tripathi, K.; Sethi, T.; Singh, A.; Tyagi, J. S. Multifaceted Remodeling by Vitamin C Boosts Sensitivity of *Mycobacterium Tuberculosis* Subpopulations to Combination Treatment by Anti-Tubercular Drugs. *Redox Biol.* **2018**, *15*, 452−466.
(59) Khameneh, B.; Bazzaz, B. S. F.; Amani, A.; Rostami, J.; Vahdati-Mashhadian, N. Combination of Anti-Tuberculosis Drugs with Vitamin C or NAC Against Different *Staphylococcus Aureus* and *Mycobacterium Tuberculosis* Strains. *Microb. Pathog.* **2016**, *93*, 83−87.
(60) Gupta, K. R.; Kasetty, S.; Chatterji, D. Novel Functions of (p)ppGpp and Cyclic di-GMP in Mycobacterial Physiology Revealed by Phenotype Microarray Analysis of Wild-Type and Isogenic Strains of *Mycobacterium smegmatis*. *Appl. Environ. Microbiol.* **2015**, *81*, 2571−2578.
(61) Gupta, K. R.; Baloni, P.; Indi, S. S.; Chatterji, D. Regulation of Growth, Cell Shape, Cell Division, and Gene Expression by Second Messengers (p)ppGpp and Cyclic di-GMP in *Mycobacterium smegmatis*. *J. Bacteriol.* **2016**, *198*, 1414−1422.
(62) Petchiappan, A.; Naik, S. Y.; Chatterji, D. RelZ-mediated Stress Response in *Mycobacterium smegmatis:* pGpp Synthesis and Its Regulation. *J. Bacteriol.* **2020**, *202*, No. e00444-19.

https://doi.org/10.1021/acsomega.3c00822
ACS Omega 2023, 8, 20513−20523

(63) Pal, A.; Ghosh, A. c-di-AMP signaling plays important role in determining antibiotic tolerance phenotypes of *Mycobacterium smegmatis*. *Sci. Rep.* **2022**, *12*, 13127.
(64) Boutte, C. C.; Crosson, S. Bacterial Lifestyle Shapes Stringent Response Activation. *Trends Microbiol.* **2013**, *21*, 174−180.
(65) Syal, K.; Flentie, K.; Bhardwaj, N.; Maiti, K.; Jayaraman, N.; Stallings, C. L.; Chatterji, D. Synthetic (p)ppGpp Analogue is an Inhibitor of Stringent Response in Mycobacteria. *Antimicrob. Agents Chemother.* **2017**, *61*, No. e00443-17.
(66) Windels, E. M.; Michiels, J. E.; Fauvart, M.; Wenseleers, T.; Van den Bergh, B.; Michiels, J. Bacterial Persistence Promotes the Evolution of Antibiotic Resistance by Increasing Survival and Mutation Rates. *ISME J.* **2019**, *13*, 1239−1251.
(67) Cohen, N. R.; Lobritz, M. A.; Collins, J. J. Microbial Persistence and the Road to Drug Resistance. *Cell Host Microbe* **2013**, *13*, 632−642.
(68) Vilchèze, C.; Hartman, T.; Weinrick, B.; Jain, P.; Weisbrod, T. R.; Leung, L. W.; Freundlich, J. S.; Jacobs, W. R., Jr. Enhanced Respiration Prevents Drug Tolerance and Drug Resistance in *Mycobacterium tuberculosis*. *Proc. Natl. Acad. Sci. U. S. A.* **2017**, *114*, 4495−4500.
(69) Hathcock, J. N.; Azzi, A.; Blumberg, J.; Bray, T.; Dickinson, A.; Frei, B.; Jialal, I.; Johnston, C. S.; Kelly, F. J.; Kraemer, K.; Packer, L.; Parthasarathy, S.; Sies, H.; Traber, M. G. Vitamins E and C are Safe Across a Broad Range of Intakes. *Am. J. Clin. Nutr.* **2005**, *81*, 736−745.
(70) Hoffer, L. J.; Levine, M.; Assouline, S.; Melnychuk, D.; Padayatty, S. J.; Rosadiuk, K.; Rousseau, C.; Robitaille, L.; Miller, W. H., Jr. Phase I Clinical Trial of i.v. Ascorbic Acid in Advanced Malignancy. *Ann. Oncol.* **2008**, *19*, 1969−1974.
(71) Stephenson, C. M.; Levin, R. D.; Spector, T.; Lis, C. G. Phase I Clinical Trial to Evaluate the Safety, Tolerability, and Pharmacokinetics of High-Dose Intravenous Ascorbic Acid in Patients with Advanced Cancer. *Cancer Chemother. Pharmacol.* **2013**, *72*, 139−146.

https://doi.org/10.1021/acsomega.3c00822
ACS Omega 2023, 8, 20513−20523